

A Resource-Driven Framework for Configurable Entanglement in Quantum Networks

Francesco Mazza, *Graduate Student Member, IEEE*, Claudio Pellitteri,
Angela Sara Cacciapuoti, *Senior Member, IEEE*, and Marcello Caleffi, *Senior Member, IEEE*

Abstract—Shared multipartite entanglement defines a “*whatever channel*”, i.e., a latent communication substrate that does not determine *a priori* which end-to-end entangled links are activated, but can be configured to support different entanglement-connectivity graphs through Local Operations and Classical Communication (LOCC). Building on this, we propose a resource-driven framework in which multipartite entanglement is treated as a *programmable resource* that induces a space of admissible entanglement-graph configurations. Within this framework, connectivity provisioning emerges as a particular instance of a more general resource reconfiguration process. To support this paradigm, we introduce a set of structural design parameters that characterize the operational degrees of freedom of the resource and define the admissible transformations independently of the specific mechanism used to realize them. We then formalize Entanglement Rolling as a measurement-based protocol that operates over the induced configuration space, enabling the systematic reconfiguration of the shared resource across a family of multipartite states. Finally, we analyze the proposed framework under realistic noise conditions. Leveraging the Noisy Stabilizer Formalism (NSF), we derive closed-form noise maps that characterize the effect of noise on the resource transformations and show that the proposed approach maintains reliable performance under relevant noise processes.

Index Terms—Quantum Internet, multipartite entanglement, quantum networks, graph states, ERC-CoG QNattyNet.

I. INTRODUCTION

The Quantum Internet [1]–[8] is expected to enable applications beyond the capabilities of classical networks, such as distributed quantum computing [9]–[11], unconditionally secure communications [12], [13], and enhanced quantum sensing [14]–[17]. At the core of this vision lies *quantum entanglement*, the fundamental resource of the network [18]–[22]. Bipartite entanglement enables point-to-point primitives such as teleportation [6], [23], while multipartite entanglement defines more general and complex communication structures [24]–[26], supporting flexible and on-demand connectivity patterns [27]–[29] beyond the constraints of the underlying physical network graph. Due to this flexibility, multipartite entanglement has been increasingly regarded as a versatile *network resource*.

The authors are with the www.QuantumInternet.it research group, University of Naples Federico II, Naples, 80125 Italy.

Corresponding author: Angela Sara Cacciapuoti, angelasara.cacciapuoti@unina.it

This work has been funded by the European Union under Horizon Europe ERC-CoG grant QNattyNet, n.101169850. Views and opinions expressed are however those of the author(s) only and do not necessarily reflect those of the European Union or the European Research Council Executive Agency. Neither the European Union nor the granting authority can be held responsible for them.

Nevertheless, the existing literature has predominantly treated multipartite entanglement as a tool for connectivity provisioning, focusing on how to distribute resources and react to sets of communication requests, as detailed in Sec. I-A. In this perspective, entanglement manipulation is typically designed to satisfy specific connectivity demands, e.g., by extracting Bell pairs or establishing end-to-end entanglement between selected nodes.

In contrast, this work adopts a different viewpoint. Rather than focusing on how to satisfy given requests, we investigate how shared multipartite entanglement can be treated as a *programmable resource* that enables the systematic instantiation of entanglement-based functionalities.

To this end, we introduce the concept of *whatever*¹ channel², namely, a shared multipartite entangled resource that does not determine *a priori* which end-to-end entangled links are instantiated, but supports the instantiation of different subsets of links through suitable operations on the shared state. In this sense, the *whatever* channel is a latent communication substrate that can be configured to realize different entanglement-connectivity patterns depending on how it is manipulated.

Building on this programmable nature of the *whatever* channel, we formalize a *resource-driven framework*, where different entanglement-based functionalities can be realized by appropriately transforming the underlying resource. More precisely, the *whatever* channel induces a well-defined space of admissible entanglement-graph configurations, rather than a fixed pattern. Accordingly, entanglement manipulation is not viewed as a one-shot extraction process, but as a structured transformation that operates over this configuration space.

To support this process, we introduce (in Sec. III) a set of structural definitions that formalize the operational degrees of freedom of the resource. These constructs provide a functional characterization, rather than a merely descriptive one, as they directly determine the admissible transformations of the resource and, consequently, the set of entanglement-graph configurations that can be instantiated. In particular, the proposed framework is not tied to a specific resource instance, but applies to a family of multipartite resource states, characterized by structural design parameters. These parameters induce the admissible transformations of the resource and

¹The authors gratefully acknowledge John D. Day for suggesting this name.

²Here, the term *channel* is not used in the conventional sense of a physical medium underlying a communication link. Rather, it denotes an entanglement-defined communication structure, in which the involved nodes may be physically distant, while still being neighbors in the entanglement connectivity graph [27].

define the corresponding space of achievable entanglement-graph configurations, independently of the mechanism used to realize them.

Within this framework, we exploit and mathematically formalize Entanglement Rolling, first introduced in [29], as a measurement-based protocol that enables the systematic reconfiguration of the shared resource across the considered family of states. Rather than acting as a mechanism for extracting specific entangled pairs, Entanglement Rolling operates over the induced configuration space, enabling its systematic exploration as a general realization mechanism. In this sense, it applies uniformly across the considered family of resource states. The Entanglement Rolling relies on a hierarchical organization of network nodes, potentially supported by control-plane coordination, and it is therefore consistent with emerging quantum network architectures [1], [2].

Since realistic quantum networks operate under decoherence, we also analyze the proposed framework under noisy conditions. By leveraging the Noisy Stabilizer Formalism [30], [31], we derive closed-form noise maps that characterize the effect of noise on the resource transformations. Furthermore, we demonstrate that the proposed approach maintains reliable performance under relevant noise processes, including depolarizing noise.

Our contributions can be summarized as follows:

- i. we introduce the concept of *whatever channel* as a shared multipartite resource and propose a *resource-driven framework* for its programmable resolution over a family of resource states;
- ii. we formalize Entanglement Rolling as a measurement-based reconfiguration protocol that operates over the induced configuration space, enabling controlled transitions among admissible entanglement-graph configurations; as a key instance, we prove that it achieves the maximum number of concurrently instantiable Bell pairs over the considered resource family;
- iii. we derive closed-form noise maps for the resource transformations induced by Entanglement Rolling, providing an analytical characterization of the framework under realistic noise;
- iv. we evaluate the performance of the proposed framework under both depolarizing and time-dependent dephasing noise, demonstrating its practical viability.

The remainder of this paper is organized as follows. A summary of the related works is provided in Sec. I-A. Sec. II provides the necessary background on multipartite entangled states and their noisy manipulation. In Sec. III, we introduce the system model and the communication paradigm of interest. Sec. IV presents the Entanglement Rolling protocol and its properties. Sec. V describes the systematic reconfiguration of the resource state through Entanglement Rolling and in Sec. VI we analyze the effect of noisy entanglement manipulation. In Sec. VII we conclude the paper.

A. Related work

Existing literature on multipartite entangled resources can be broadly grouped along two main directions: i) gener-

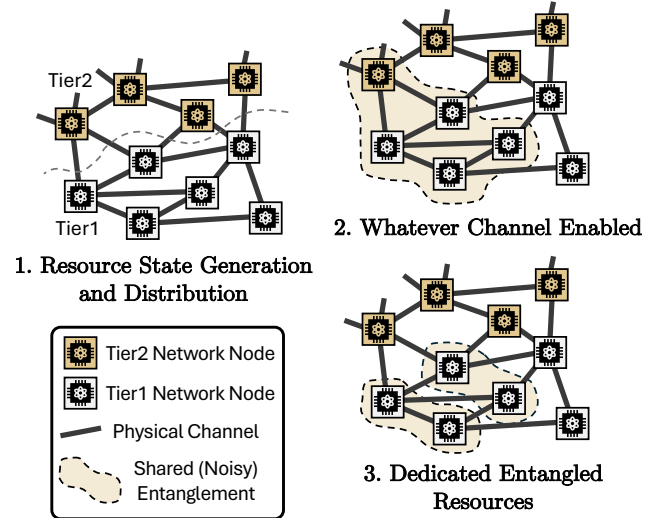


Fig. 1: High level representation of our research problem. The generation and distribution of a multipartite resource state (1) establishes a *whatever channel* between a subset of network nodes (2). By applying LOCC operations on the shared resource state, entanglement can be reconfigured and shared between a subset of network nodes (3), for instance, parallel communication resources can be extracted through the resolution of the *whatever channel*.

ation and distribution; ii) utilization for connectivity provisioning. Regarding the first direction, a substantial body of literature addresses how multipartite resource states can be generated and distributed over quantum networks, with performance largely dominated by technological constraints and network scale. Representative approaches include graph-state generation via quantum emitters [32], [33] and fusion operations [34]–[36], as well as network-level distribution mechanisms encompassing purification, and repeater-based schemes [7], [37], [38].

Regarding instead the second direction, multipartite resources have been extensively studied as *connectivity-provisioning* tools, where local operations reshape the resource to satisfy point-to-point entanglement requests [39], [40]. In this context, graph and cluster states [41], [42] have emerged as the predominant resource models, as they provide a convenient representation that enables structured manipulation and analytical tractability. This perspective underlies a wide range of works on Bell-pair routing [43], quantum repeater architectures [7], [37], [38], and resource allocation across network scales [2], [25], [29], [44]–[46].

The present work departs from the above perspectives in a fundamental way: rather than treating graph-state manipulation as a means to satisfy predefined connectivity requests, we consider multipartite entanglement as a programmable resource that induces a space of admissible configurations. In this view, connectivity provisioning becomes one possible outcome of a more general resource reconfiguration process. Accordingly, our goal is to define a resource-driven framework that characterizes how a shared multipartite state can be systematically

reconfigured. Within this framework, mechanisms such as Entanglement Rolling provide a concrete way to operate over the induced configuration space.

II. PRELIMINARIES

Here, we introduce graph states and the Noisy Stabilizer Formalism (NSF), the two mathematical tools used throughout the paper to model and manipulate noisy resources.

A graph state $|G\rangle$ is associated to a graph $G = (V, E)$, where V is the set of vertices and E is the set of edges. To each vertex of the graph corresponds a qubit, and the entanglement between different qubits is represented by the application of a controlled- Z gate, thus encoding the edges of the graph. The formalism of graph states allows for a straightforward description of entanglement relations between subsystems as well as a natural way of describing their manipulations, as detailed in [41], [42]. Interestingly, graph states are stabilizer states: $|G\rangle$ is the unique common $+1$ eigenstate of an associated stabilizer group.

Definition 1 (Stabilizer Operators of Graph States). *The stabilizer operators $\{K_a\}_{a \in V}$ of an n -qubit graph state $|G\rangle$, associated with the graph $G = (V, E)$, are the n commuting Hermitian n -qubit Pauli operators satisfying $K_a|G\rangle = |G\rangle$, for all $a \in V$ with*

$$K_a = X_a \prod_{b \in N_a} Z_b, \quad (1)$$

where X_a and Z_b denote the Pauli X and Z operators acting on qubits a and b respectively, and $N_a \subseteq V$ denotes the neighborhood of vertex a in G .

Remark. The symbol $U_j \in \{\mathbb{I}_j, X_j, Y_j, Z_j\}$ implicitly refers to the application of identity operators to all qubits except j :

$$U_j = (\mathbb{I}^{(1)} \otimes \dots \otimes U^{(j)} \otimes \dots \otimes \mathbb{I}^{(n)}). \quad (2)$$

The application of specific local unitaries and single-qubit Pauli measurements on a graph state yields, up to local corrections, another graph state. The corresponding transformation can be described directly at the level of the underlying graph via simple graph operations. These operations can be concisely described by a *manipulation operator* \mathbf{O} (e.g. a Pauli measurement on qubit (a) $\mathbf{M}_\xi = \langle \xi, \pm |^{(a)} \otimes (U_{\xi, \pm}^{(a)})^\dagger P_{\xi, \pm}^{(a)}$, with $\xi \in \{x, y, z\}$ or a local complementation unitary), applied to the graph state $|G\rangle$ to obtain a new graph state $|G'\rangle$. We refer the readers to [41], [42] for a detailed discussion on the correspondence between local operations on graph states and their resulting associated graph.

The Noisy Stabilizer Formalism (NSF) is a powerful method to describe the manipulation of noisy graph states [30], [31]. Specifically, instead of applying manipulation operators directly to a noisy graph state, NSF allows the application of manipulation operators to the underlying pure state $\varrho = |G\rangle\langle G|$, while updating the noise maps acting on the state. Thanks to the noisy stabilizer formalism, the noise operators \mathbf{N}_j of each (Pauli) noise map \mathcal{M}_j can be updated up to recurrent commutation rules, depending on the applied manipulation operator \mathbf{O}_i . Suppose we apply a set of manipulation operators

| Operator \mathbf{O} on qubit a | Updated j -th Noise operator |
|------------------------------------|--|
| $\mathbf{M}_{z, \pm}^{(a)}$ | $\tilde{\Lambda}_j = \begin{cases} \prod_{k \in N_a} Z_k^\beta & \text{if } j = a \\ Z_j^\alpha \prod_{k \in N'_j} Z_k^\beta & \text{otherwise} \end{cases}$ |
| $\mathbf{M}_{y, \pm}^{(a)}$ | $\tilde{\Lambda}_j = \begin{cases} \prod_{k \in N_a} Z_k^{\alpha+\beta} & \text{if } j = a \\ Z_j^{\alpha+\beta} \prod_{k \in N'_j} Z_k^\beta & \text{if } j \in N_a \\ Z_j^\alpha \prod_{k \in N'_j} Z_k^\beta & \text{otherwise} \end{cases}$ |
| $\mathbf{M}_{x, \pm}^{(a)}$ | $\tilde{\Lambda}_j = \begin{cases} Z_{b_0}^\alpha \prod_{k \in N_{b_0}} Z_k^\alpha & \text{if } j = a \\ Z_{b_0}^\beta \prod_{k \in N'_{b_0}} Z_k^\alpha & \text{if } j = b_0 \\ Z_j^\alpha \prod_{k \in N'_j} Z_k^\beta & \text{otherwise} \end{cases}$ |

TABLE I: Updating rules for Pauli noise operators corresponding to the application of operator \mathbf{O} on qubit a . Here N'_j denotes the neighborhood of qubit j in the graph *after* the application of \mathbf{O} . The exponents $\alpha, \beta \in \{0, 1\}$ are binary indices with $Z^0 = \mathbb{I}$ and $Z^1 = Z$. Table reproduced from [30].

$\mathcal{O} = \{\mathbf{O}_1, \dots, \mathbf{O}_k\}$ to the noisy graph state $\mathcal{M}_n \dots \mathcal{M}_1 \varrho$. The resulting state is given by:

$$(\mathbf{O}_k \dots \mathbf{O}_1) \mathcal{M}_n \dots \mathcal{M}_1 \varrho (\mathbf{O}_1^\dagger \dots \mathbf{O}_k^\dagger). \quad (3)$$

Thanks to the NSF, this can be equivalently written as:

$$\tilde{\mathcal{M}}_n \dots \tilde{\mathcal{M}}_1 (\mathbf{O}_k \dots \mathbf{O}_1) \varrho (\mathbf{O}_1^\dagger \dots \mathbf{O}_k^\dagger), \quad (4)$$

where $(\mathbf{O}_k \dots \mathbf{O}_1) \varrho (\mathbf{O}_1^\dagger \dots \mathbf{O}_k^\dagger) = \varrho'$ is the noiseless manipulated graph state, according to manipulation operators \mathbf{O}_i with $i \in \{1, \dots, k\}$, and $\tilde{\mathcal{M}}_j$ is the *updated* noise map, with $j \in \{1, \dots, n\}$. Consequently, the resulting noisy graph given by the action of independent single-qubit noises is given by the application of multiple maps: $\tilde{\mathcal{M}}_n \dots \tilde{\mathcal{M}}_1 \varrho'$. As a result, each updated noise map on a qubit j is composed by updated noise operators $\tilde{\Lambda}_{j, \alpha \beta}$ whose update is completely described by recurrent commutation rules with respect to the applied operation [30], and explicitly reported in Tab. I for Pauli measurements.

III. SYSTEM MODEL: RESOURCE-DRIVEN ENTANGLEMENT RECONFIGURATION

We consider a quantum network in which a set of nodes share a multipartite entangled resource state. As discussed in Sec. I, such a resource defines a *whatever channel*, i.e., a programmable communication substrate that can be configured to realize different entanglement-connectivity patterns through LOCC. Indeed, the shared entanglement induces a space of admissible entanglement-graph configurations, determined by its structure and by the allowed set of local operations. Within this space, different configurations correspond to different realizable connectivity patterns among subsets of nodes.

Whatever Channel Resolution. Given a whatever channel, its *resolution* is the selection and instantiation of a specific entanglement-graph configuration from the admissible space, through LOCC applied to qubits stored at the network nodes.

A key problem is therefore to characterize and systematically explore such a configuration space. In particular, we

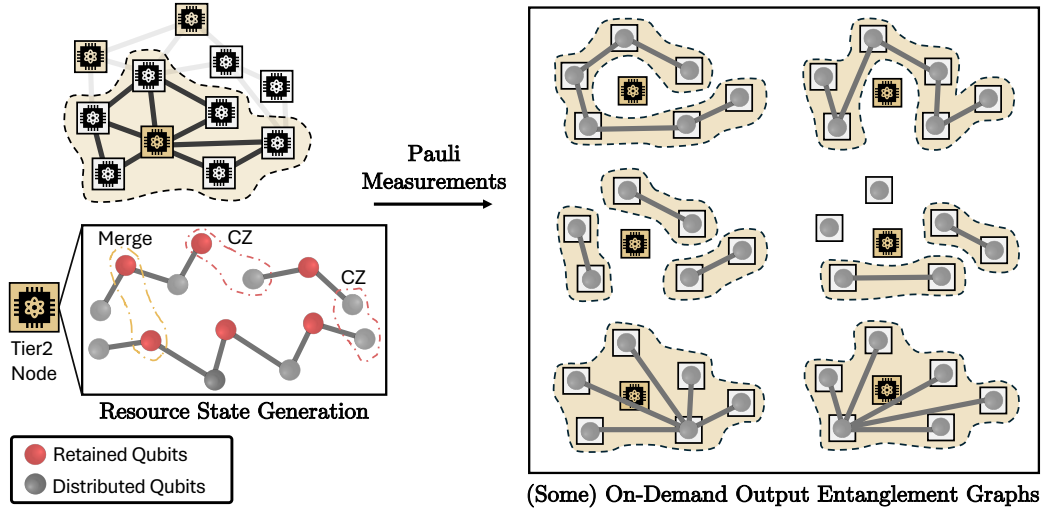


Fig. 2: Pictorial representation of the system model and node hierarchy. Tier2 node(s) retains n_o orchestration qubits V_o of a shared two-colorable graph state, while the κ peer qubits V_c are distributed to Tier1 nodes.

aim to identify: (i) the *structural properties* of the resource state that determine the admissible transformations, and (ii) the *mechanisms* that enable the controlled realization of useful configurations within that space.

Importantly, these two aspects are conceptually decoupled. The resource structure determines the constraints and the set of achievable configurations, independently of the realization mechanism. In contrast, concrete protocols operate over the induced space, by providing explicit procedures to transform the resource to satisfy specific tasks and network requests. In the following, we formalize this perspective by introducing a set of structural design parameters that characterize the resource and its admissible transformations, and by defining the operational model used to manipulate the shared entanglement.

A. System Model and Communication Paradigm

Whatever channel resolution is not tied to a unique realization. In general, an arbitrary multipartite resource may induce an opaque space of admissible entanglement-connectivity configurations. For generic graph states, explicitly characterizing this space or even determining a systematic reduction to disjoint Bell states becomes quickly intractable [40]. For this reason, we adopt a *resource-engineering* perspective: rather than assuming an arbitrary shared state, we focus on *parametrized* resource families, whose structure exposes controllable degrees of freedom. This yields an explicit characterization of the configuration space induced by the shared resource, enabling systematic control and providing a foundation to realize multiple entanglement-based functionalities via resource reconfiguration.

To this end, we introduce *Generalized Tree-like* (GTL) graph states, a family of two-colorable graph states with proven networking applications [29], [47]. GTL states are specified by structural design parameters that capture their topology and determine the admissible entanglement transformations they support. Their intrinsic bipartite structure induces a natural partition of qubits into two disjoint vertex sets,

$V = V_o \cup V_c$, $V_o \cap V_c = \emptyset$, which we interpret operationally through a *hierarchical network model*.

In fact, emerging Quantum Internet architectures distinguish network nodes in terms of computational resources and functional responsibilities [1], [2]. In particular, *Tier2 nodes* are high-capability devices that host and manipulate multipartite resources, whereas *Tier1 nodes* are resource-constrained devices, that primarily apply local corrections and consume the provided entanglement.

Within this model, Tier2 nodes collectively retain the qubits in V_o , termed *orchestration qubits*, of a shared two-colorable graph state, while Tier1 nodes receive the distributed qubits in V_c , termed *peer qubits*. Each Tier2 node can perform local Pauli measurements on its orchestration qubits independently, triggering the desired entanglement manipulation, regardless of how the remaining orchestration qubits are distributed among other Tier2 nodes. The resulting entanglement manipulation is coordinated across Tier2 nodes and delivered to Tier1 nodes through LOCC, yielding on-demand entanglement links among selected utilizers, as depicted in Fig. 2.

We note that the adopted *hierarchical network model* is *scale-adaptable*. Depending on the deployment, it can describe large-scale tiered architectures with multiple Tier2 nodes as in [2], or compact settings in which a single node concentrates Tier2 functionality. Accordingly, all definitions, theorems, and results in this manuscript are independent of the number of Tier2 nodes. As a concrete example, a Quantum Local Area Network (QLAN) [29], [47] instantiates the same hierarchy at small scale, where a single orchestrator acts as the Tier2 node and the serving nodes act as Tier1 nodes.

B. Resource State Design Parameters

To ensure practical realizability, we focus on two-colorable graph-state resources, which admit modular constructions from elementary one-dimensional (1D) cluster states via suitable

merging operations³ [32], [34], [35].

Let $G = (V, E)$ be the graph associated with the distributed two-colorable resource state. Its vertex set is partitioned in two disjoint subsets $V_o = \{o_1, \dots, o_{n_o}\}$ and $V_c = \{c_1, \dots, c_\kappa\}$, where $|V_o| = n_o$ denotes the number of *orchestration qubits* retained by the Tier2 node(s) and $|V_c| = \kappa$ represents the number of *peer qubits* distributed to Tier1 nodes. Accordingly, the total number of qubits is $n = n_o + \kappa$. The number of Tier1 nodes is at most κ (one qubit per node), but can be smaller if some Tier1 nodes hold multiple peer qubits.

Following [29], we characterize the considered resource family through a small set of structural parameters that determine the structure and the admissible entanglement transformations. In particular, we distinguish *peer degree*, the *bridge rank* and *bridge degree*.

Definition 2 (r-rank bridge). An *r-rank bridge* b_i is a peer qubit adjacent to $\mathbf{r} > 1$ orchestration qubits. The set of *r-rank bridges* is formally defined as:

$$\mathcal{B}_r = \{b_i \in V_c : |N_{b_i} \cap V_o| = \mathbf{r}\}, \text{ with } \mathbf{r} > 1. \quad (5)$$

Definition 3 (Bridge degree). The *bridge degree* $\kappa_{b,r}^{(o_i)} \leq \kappa$ of an orchestration qubit $o_i \in V_o$ with respect to rank \mathbf{r} is the number of *r-rank bridges* $b_i \in \mathcal{B}_r$ belonging to its neighborhood N_{o_i} :

$$\kappa_{b,r}^{(o_i)} = |\mathcal{B}_r \cap N_{o_i}|, \quad o_i \in V_o, \quad (6)$$

For brevity, when $\mathbf{r} = 2$, we write $\mathcal{B} \equiv \mathcal{B}_2$ and $\kappa_b^{(o_i)} \equiv \kappa_{b,2}^{(o_i)}$.

Definition 4 (Peer degree). The *peer degree* $\kappa_c^{(o_i)} \leq \kappa$, of an orchestration qubit $o_i \in V_o$ is the number of adjacent peer qubits:

$$\kappa_c^{(o_i)} = |N_{o_i} \cap V_c|, \quad o_i \in V_o. \quad (7)$$

We focus on *regular* resource structures, where the bridge rank \mathbf{r} is fixed across the topology (thus, the subscript will be omitted for notation simplification) and each orchestration qubit has either minimum bridge degree $\hat{\kappa}_b$ or maximum bridge degree $\bar{\kappa}_b$. Formally:

$$\hat{\kappa}_b = \min_{o_i \in V_o} \{\kappa_b^{(o_i)}\}, \quad \bar{\kappa}_b = \max_{o_i \in V_o} \{\kappa_b^{(o_i)}\} = 2\hat{\kappa}_b. \quad (8)$$

One of the simplest graph states that can be defined according to these parameters is the *chain graph state* [29], which is characterized by a 1D linear graph state structure with $\kappa_c = 2 = \bar{\kappa}_b$, $\hat{\kappa}_b = 1$, and $\mathbf{r} = 2$. The fundamental resource family considered in this work is the *Generalized Tree-like* (GTL) graph state, obtained by fixing $\mathbf{r} = 2$.

Definition 5 (Generalized Tree-like (GTL)). An *n-qubit GTL graph state* is a tuple

$$\text{GTL} = (G, \kappa_c, \hat{\kappa}_b), \quad \kappa_c, \hat{\kappa}_b \in \mathbb{N}^+, \quad \kappa_c \geq 2\hat{\kappa}_b, \quad (9)$$

where $G = (V, E)$ is a two-colorable graph with vertex bipartition $V = V_o \cup V_c$, satisfying the following structural constraints:

³A merging operation between two vertices of different graph states combines them into a single vertex. In the optical graph-states literature this is often referred to as fusion.

- C1.** (Peer degree regularity) $|N_{o_i} \cap V_c| = \kappa_c$ for every $o_i \in V_o$, with κ_c the peer degree in Def. 4.
- C2.** (Linear bridge ordering) V_o carries a linear order, every bridge $b \in \mathcal{B}$ (Def. 2) is adjacent to exactly one consecutive pair (o_j, o_{j+1}) .
- C3.** (Bridge regularity) each consecutive pair (o_j, o_{j+1}) shares exactly $\hat{\kappa}_b$ bridges, with $\hat{\kappa}_b$ the minimum bridge degree in Def. 3.

From **C2–C3**, boundary orchestration qubits (o_1, o_{n_o}) have bridge degree $\hat{\kappa}_b$, interior ones have bridge degree $\bar{\kappa}_b = 2\hat{\kappa}_b$. Moreover, the number of orchestration qubits is $n_o = \frac{\kappa - \hat{\kappa}_b}{\kappa_c - \hat{\kappa}_b}$, with $n = n_o + \kappa$.

Within the configuration space induced by the GTL resource family, useful entanglement-connectivity patterns should target the following practically meaningful goals:

- *Entanglement link formation* – enabling entanglement links between non-neighbor endpoints, by reducing the number of intermediate hops separating them in the resource graph;
- *Parallel resource instantiation* – maximizing the number of disjoint resources (Bell pairs or GHZs or other communication resources) that can be concurrently instantiated from the shared resource;
- *Hierarchy compliance* – any realization mechanism must operate within the hierarchical responsibility model, with configurable operations confined to Tier2 nodes and requiring no inter-node coordination among Tier1 nodes.

The regime $\kappa_c > 2\hat{\kappa}_b$ yields additional non-bridge peer qubits that do not increase the number of concurrently instantiable entangled resources, offering no practical advantages for the above goals. Thus, for the remainder of this manuscript, we focus on the subclass $\kappa_c = 2\hat{\kappa}_b$. Under this restriction κ_c is fully determined by $\hat{\kappa}_b$, and the GTL reduces to the two-parameter tuple

$$\text{GTL} = (G, \hat{\kappa}_b), \quad \hat{\kappa}_b \in \mathbb{N}^+, \quad \hat{\kappa}_b \geq 2, \quad (10)$$

for which the number of orchestration qubits is $n_o = (\kappa - \hat{\kappa}_b)/\hat{\kappa}_b$.

In the following, we show how to achieve all three aforementioned goals within the induced configuration space via a mechanism termed Entanglement Rolling.

IV. ENTANGLEMENT ROLLING

Here, we formalize Entanglement Rolling as a systematic procedure to navigate through the configuration space of the GTL resource family to engineer entanglement-graph configurations.

A. Proximity and bridge neighborhoods

Sharing tailored resource states in a quantum network mitigates the limitations imposed by the physical network graph: even if endpoints are not connected by a physical link, they may become neighbors in the overlaid entanglement graph induced by the shared resource. In the GTL family, this entanglement graph is two-colorable, with bipartition $V = V_o \cup V_c$. Hence, peer qubits $c_i, c_j \in V_c$ are never adjacent,

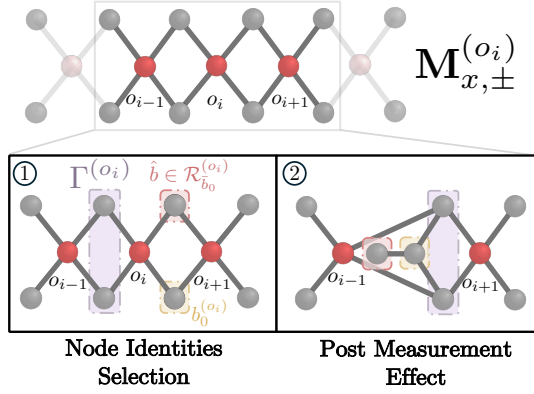


Fig. 3: Illustration of the Entanglement Rolling effect induced by a Pauli X measurement on orchestration qubit o_i of a GTL resource state $(G, \hat{\kappa}_b = 2)$ with arbitrary length.

and any path between them necessarily alternates between peer and orchestration vertices. Accordingly, to quantify how “far” two peer qubits are, we measure their distance in terms of the *bridges* encountered along a shortest path. Cor. 1 shows that this metric directly matches the number of Entanglement Rolling steps needed to establish an entangled link between the selected peer vertices.

Definition 6 (Peer proximity). *The peer proximity $\pi(c_i, c_j)$ between two peer qubits $c_i, c_j \in V_c \subset V$ with $i \neq j$, is defined as one plus the number of bridges on a shortest path p_{c_i, c_j} , between them in $G = (V, E)$:*

$$\pi(c_i, c_j) = 1 + |\beta_{c_i, c_j}|, \quad (11)$$

with $\beta_{c_i, c_j} = \{b \in p_{c_i, c_j} : b \in \mathcal{B}\}$ denoting the set of bridges along the shortest path p_{c_i, c_j} .

To better capture the engineering role of bridges in our framework, we define the *bridge neighborhoods*, which partition the rank- $r = 2$ bridges of an orchestration vertex into two sets.

Definition 7 (Bridge neighborhoods). *Given an orchestration vertex $o_i \in V_o$, its rank- $r = 2$ bridge neighbors can be partitioned in two disjoint sets: the left bridge neighborhood $\mathcal{L}_B^{(o_i)}$ and the right bridge neighborhood $\mathcal{R}_B^{(o_i)}$, defined as*

$$\mathcal{R}_B^{(o_i)} = \begin{cases} \mathcal{B}^{(o_i)} \cap \mathcal{B}^{(o_{i+1})} & \text{if } o_{i+1} \in V_o \\ \emptyset & \text{otherwise} \end{cases}, \quad (12)$$

$$\mathcal{L}_B^{(o_i)} = \begin{cases} \mathcal{B}^{(o_i)} \cap \mathcal{B}^{(o_{i-1})} & \text{if } o_{i-1} \in V_o \\ \emptyset & \text{otherwise} \end{cases}. \quad (13)$$

By C2 of Def. 5, $\mathcal{L}_B^{(o_i)}$ and $\mathcal{R}_B^{(o_i)}$ are disjoint, and by C3 each non-empty set has cardinality $\hat{\kappa}_b$.

B. Entanglement Rolling Effect

Theorem 1 formalizes the *Entanglement Rolling Effect* induced by a Pauli X measurement on an orchestration qubit o_i with a freely chosen support vertex $b_0^{(o_i)}$. This single-step

effect is the elementary building block of the *Entanglement Rolling procedure*: repeating this operation over a subset of the n_o orchestration qubits, according to a configurable support vertex sequence $\mathcal{S}_{b_0} = \{b_0^{(o_1)}, \dots, b_0^{(o_{n_o})}\}$, yields the *Entanglement Rolling procedure*, which progressively reduces the entanglement proximity among selected endpoints.

Theorem 1 (Entanglement Rolling Effect). *Given a distributed n -qubit GTL graph state in a quantum network with n_o orchestration qubits and κ peer qubits, a Pauli X measurement – described by the manipulation operator $M_{x, \pm}^{(o_i)}$ – is applied on the orchestration qubit $o_i \in V_o$ with support vertex $b_0^{(o_i)}$. The measurement induces an Entanglement Rolling effect:*

- i.) *The designated vertex $b_0^{(o_i)}$ becomes the center of a star connecting all neighbors of the measured vertex o_i .*
- ii.) *Peer qubits in $\Gamma^{(o_i)} = N_{o_i} \setminus \mathcal{R}_B^{(o_i)}$ become neighbors of the next orchestration qubit o_{i+1} , whenever o_{i+1} exists.*

Proof. Please refer to Appendix A for the proof. \square

Remark. Th. 1 is stated for $b_0^{(o_i)} \in \mathcal{R}_B^{(o_i)}$, but holds symmetrically for $b_0^{(o_i)} \in \mathcal{L}_B^{(o_i)}$ by reversing the ordering of orchestration qubits.

A pictorial representation of the results in Th. 1 is provided in Fig. 3, where b_0 and the set of rolled vertices $\Gamma^{(o_i)}$ are highlighted before and after the measurement. A direct consequence of Th. 1 is the reduction of entanglement proximity, not only for a target vertex c_j , but also for all vertices selected as support vertices. This is a key feature of the entanglement rolling effect, since it can be exploited to properly generate desired entanglement links by appropriately selecting the support vertices. This proximity-reduction behavior was first observed in [29] for specific QLAN-oriented instances. We restate it here in the GTL parametrized model to extend the result to the entire resource family and to keep the paper self-contained, as it underpins the subsequent configuration-space and resource-instantiation analysis. Indeed, the proximity-reduction result follows from Th. 1, by assuming a constant set of rolled vertices $\Gamma^{(o_i)}$ at each measurement step.

Corollary 1 (Entanglement Rolling: Proximity Reduction). *Consider a distributed n -qubit GTL graph state with κ peer qubits. Two peer qubits $c_i, c_j \in V_c$, $i \neq j$, can be made adjacent in the entanglement graph by performing $\pi(c_i, c_j)$ Pauli X measurements on orchestration qubits belonging to the shortest path p_{c_i, c_j} connecting c_i and c_j in G .*

Proof. The proof follows by iterating $\pi(c_i, c_j)$ Pauli X measurement steps described in Th. 1, with $\pi(c_i, c_j)$ defined in Def. 6. At each step the rolled set becomes adjacent to the subsequent orchestration vertex, if any. By choosing the support-vertex sequence \mathcal{S}_{b_0} such that the rolled set remains constant at every measurement step, i.e., $\Gamma = \Gamma^{(o_i)}, \forall o_i \in V_o$, the proximity $\pi(c_i, c_j)$ decreases by 1 at each measurement until the two peer qubits c_i and c_j become adjacent in the entanglement graph. For an alternative derivation, please refer to [29]. \square

V. WHATEVER CHANNEL RESOLUTION VIA ENTANGLEMENT ROLLING

This section completes the *whatever-channel resolution* pipeline introduced in Sec. III. In our framework, resolution is a structured LOCC process that selects a target entanglement-graph configuration from the admissible space induced by the resource and then realizes it. Entanglement Rolling implements the Tier2-side navigation of this space, while a second stage of local Tier1 operations isolates the desired end-to-end resources.

A. Two-Stage Resolution

When a GTL graph state is distributed in the network, resolution proceeds in two stages as an LOCC process that instantiates a target entanglement-graph configuration from the admissible space, as depicted in Fig. 4.

Stage 1 (Tier2 configuration selection). Tier2 node(s) apply a configurable sequence of Pauli X measurements on orchestration qubits in V_o , implementing Entanglement Rolling and steering the shared resource toward a target entanglement-graph configuration (Th. 1, Cor. 1). Depending on which orchestration qubits are measured, the instantiated configuration may be *pure-peer* (an entanglement graph supported only on V_c) or *hybrid* (retaining a subset of unmeasured orchestration qubits and thus retaining Tier2 vertices in the instantiated entanglement graph).

Once a configuration has been instantiated, further LOCC manipulations can be applied *on top* of it to realize specific entanglement-based functionalities. In particular, when the objective is to isolate end-to-end links between peer endpoints, *Stage 2* applies a local *isolation step* at Tier1 nodes: selected peer qubits are measured in the Pauli- Z basis to remove undesired vertices and obtain disjoint entanglement resources (e.g., Bell pairs or GHZ states) from the instantiated configuration. These operations are purely local and require no inter-node quantum coordination among Tier1 nodes, which rely on classical side information produced during Stage 1 and handled by the control plane [2], [3].

In the remainder of this section, we focus on pure-peer resolutions followed by Tier1- Z stage, for isolating the desired end-to-end resources.

Remark (Architectural trade-off). The Tier1 isolation stage is not a mandatory component of whatever-channel resolution, but an architectural choice. A fully centralized alternative is to concentrate all measurements at Tier2: as shown in [29], performing n_o Pauli measurements with $\xi \in \{y, z\}$ (instead of X) directly yields n_o independent Bell pairs, without any Tier1 Pauli Z measurements. This centralization simplifies Tier1 at the cost of reduced reconfigurability, since the achievable patterns are constrained to pairs at entanglement proximity $\pi = 1$ in the initial resource state. In contrast, our two-stage design trades a lightweight local Tier1 post-processing for increased configurability, enabling the systematic instantiation of a broader set of entanglement-graph configurations.

In our approach, Tier1 nodes receive two types of classical messages. (i) After each Pauli X measurement on o_i , Tier2 disseminates outcome-dependent correction instructions to the

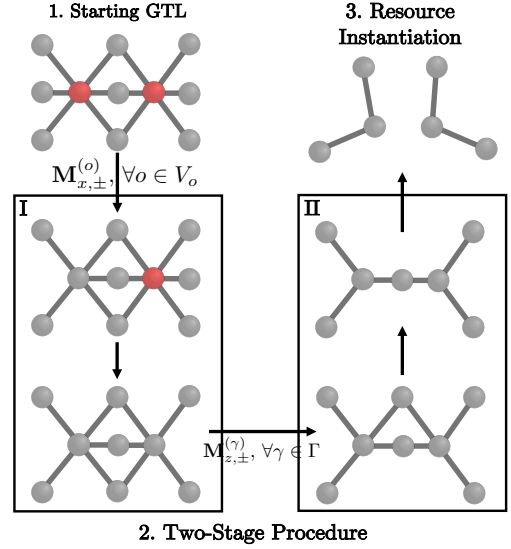


Fig. 4: Example resource state extraction using the Entanglement Rolling procedure on a GTL resource state ($G, \hat{\kappa}_b = 3$): a configurable sequence of Pauli X measurements at Tier2, followed by local Pauli Z measurements at the Tier1 end-node level, extracts two independent entangled resources (LU equivalent to 3-qubit GHZ states).

peer qubits in N_{o_i} ; the designated support vertex $b_0^{(o_i)}$ receives a different correction than the remaining neighbors [42], [47]. This asymmetry identifies the chosen support vertex $b_0^{(o_i)}$ and can be handled via standard Pauli-frame tracking. (ii) After the completion of Stage 1, Tier1 nodes receive *isolation* directives specifying which additional local Pauli Z measurements to perform to obtain the desired disjoint resources.

The selection of which resources to isolate (and when) depends on scheduling and policy decisions, including traffic patterns and control-plane objectives. These aspects are delegated to the control-plane/Tier2 interaction and a full treatment of such policies is left for future work. Here, we focus on the underlying resolution mechanism and assume that Tier1 nodes simply execute the received local directives without inter-node coordination. Overall, the sequence $\mathcal{S}_{b_0} = \{b_0^{(o_1)}, \dots, b_0^{(o_{n_o})}\}$ captures the software-defined configuration of the whatever-channel resolution, while the non-support bridges are formally defined as:

$$\bar{\mathcal{S}}_{b_0}^{(o_k)} = \begin{cases} \mathcal{R}_{b_0}^{(o_k)} & \text{if } b_0^{(o_k)} \in \mathcal{R}_B^{(o_k)} \\ \mathcal{L}_{b_0}^{(o_k)} & \text{if } b_0^{(o_k)} \in \mathcal{L}_B^{(o_k)} \end{cases}. \quad (14)$$

B. Representative Instance: Maximal parallel Bell Pairs

The proposed resource-driven framework supports multiple resolution objectives within the induced configuration space. As a key instance, we consider *maximal parallel Bell-pair instantiation*, i.e., maximizing the number of disjoint Bell pairs that can be isolated concurrently from a distributed GTL state. Thanks to Entanglement Rolling, the maximum number of concurrently instantiable Bell pairs can be achieved by measuring (in Stage 1) the orchestration qubits via a suitable

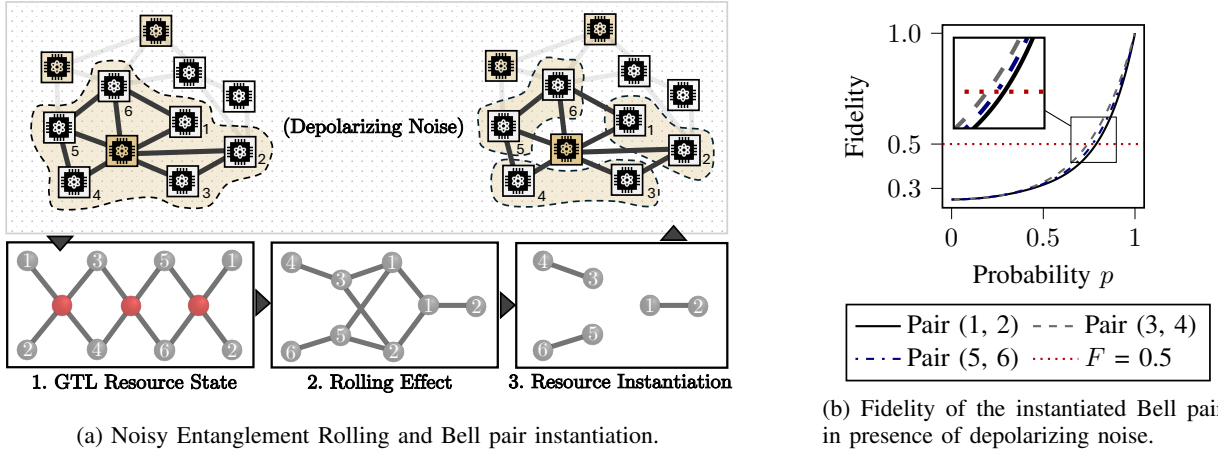


Fig. 5: Example of (a) Entanglement Rolling with noisy GTL graph state $(G, \hat{\kappa}_b = 2)$. Node labels denote Tier1 nodes; repeated labels indicate that the same Tier1 node holds multiple peer qubits, as the general case discussed in Sec. III. Pauli X measurements at Tier2, followed by local Pauli- Z measurements at Tier1, isolate independent Bell pairs under depolarizing noise (b) Fidelity of the extracted Bell pairs vs. the depolarizing parameter p (one curve per extracted pair).

Pauli X measurement sequence and then (in Stage 2) applying additional local Pauli Z measurements at Tier1 nodes to isolate disjoint pairs, as formalized below.

Corollary 2 (Entanglement Rolling: Maximal Parallel Bell-Pair Instantiation). *Consider a distributed n -qubit GTL graph state in a quantum network with n_o orchestration qubits in the operating regime $\hat{\kappa}_b \geq 2$. It is possible to instantiate the maximum number n_o of disjoint Bell pairs concurrently, by performing a total of n_o Pauli- X measurements on the orchestration qubits, followed by $\hat{\kappa}_b + n_o(\hat{\kappa}_b - 2)$ local Pauli- Z measurements on peer qubits.*

Proof. Please refer to Appendix B for the proof. \square

After Stage 1, the intermediate output is a collection of n_o disconnected star graph states, each LU-equivalent to a $\hat{\kappa}_b$ -qubit GHZ state (see Fig. 4). For $\hat{\kappa}_b = 2$, the stars are already LU-equivalent to Bell pairs and no further measurements are needed. For $\hat{\kappa}_b \geq 3$, each star requires $\hat{\kappa}_b - 2$ additional Tier1 Pauli Z measurements to isolate a Bell pair.

VI. NOISE ANALYSIS AND PERFORMANCE EVALUATION

In this section, we analyze the proposed framework under realistic noise conditions. Leveraging the NSF introduced in Sec. II, we derive closed-form noise maps that characterize how quantum noise propagates through the *resource transformations* induced by Entanglement Rolling and by the subsequent local isolation steps. Importantly, these expressions depend on the local operations applied to the resource and on the noise models, rather than on how the orchestration qubits are partitioned across Tier2 nodes. Consequently, the derivation applies unchanged to deployments with one or multiple Tier2 nodes. Accordingly, for the performance evaluation, we instantiate the framework in a practically relevant tiered deployment in which a single Tier2 node distributes the GTL resource to multiple Tier1 nodes within a QLAN [29], [47], [48]. This choice simplifies the distribution phase by

construction – which is not the focus of this paper – while preserving the generality of the entanglement manipulation process supported by our framework.

We consider two main sources of noise acting on single qubits: (i) depolarizing Pauli noise \mathcal{D} , modeling the worst-case imperfections in resource generation and distribution, and (ii) a time-dependent dephasing noise $\mathcal{F}(t)$, modeling memory decoherence during the manipulation process, similarly to the approach in [49].

A. Noisy Entanglement Manipulation

A depolarizing Pauli noise acting on qubit a of a graph state ρ can be expressed in terms of Z -type operators only:

$$\mathcal{D}_a(\rho) = p\rho + \frac{1-p}{4} \sum_{\alpha, \beta \in \{0,1\}} (Z_a^\alpha \prod_{b \in N_a} Z_b^\beta) \rho (Z_a^\alpha \prod_{b \in N_a} Z_b^\beta). \quad (15)$$

The use of the NSF allows to update the noise operators after the application of manipulation operators. More specifically, if we consider the application of Entanglement Rolling or an arbitrary measurement strategy, the following manipulation operators are applied to the orchestration qubits:

$$\mathcal{O}_\xi = \{\mathbf{M}_{\xi, \pm}^{(o_1)}, \mathbf{M}_{\xi, \pm}^{(o_2)}, \dots, \mathbf{M}_{\xi, \pm}^{(o_{n_o})}\}, \text{ with } \xi \in \{x, y, z\}, \quad (16)$$

where the measurement operators are applied on the quantum state from left to right. If we consider that each qubit is independently affected by a depolarizing Pauli noise \mathcal{D}_j , the distributed noisy graph state is: $\mathcal{D}_1 \dots \mathcal{D}_n |G\rangle \langle G|$, with $n = n_o + \kappa$. The NSF update rules reported in Tab. I, allow us to commute the noise through the measurement sequence, resulting in *updated* local noise maps $\tilde{\mathcal{D}}_j$ acting on the post-measurement state. The next proposition provides closed-form expressions for the resulting updated depolarizing noise maps on peer and orchestration qubits.

Proposition 1. *Consider a noisy GTL graph state $(G, \hat{\kappa}_b)$ with $\hat{\kappa}_b \geq 2$, affected by independent single-qubit depolarizing*

channels, and the ordered Entanglement-Rolling measurement sequence $\mathcal{O}_x = \{\mathbf{M}_{x,\pm}^{(o_1)}, \dots, \mathbf{M}_{x,\pm}^{(o_{n_o})}\}$. Using the NSF, one can update each local depolarizing channel separately. In particular, the updated depolarizing map associated with a noisy peer qubit $c_j \in N_{o_i}$ is given by:

$$\begin{aligned} \tilde{\mathcal{D}}_{c_j}(\varrho) = & p\varrho + \frac{(1-p)}{4} \left[\varrho + Z_{c_j} \varrho Z_{c_j} + \left(\prod_{k \in \tilde{N}} Z_k \right) \varrho \left(\prod_{k \in \tilde{N}} Z_k \right) + \right. \\ & \left. + \left(Z_{c_j} \prod_{k \in \tilde{N}} Z_k \right) \varrho \left(Z_{c_j} \prod_{k \in \tilde{N}} Z_k \right) \right], \end{aligned} \quad (17)$$

where ϱ is the noiseless post-measurement graph state and the set \tilde{N} depends on the type of peer qubit c_j :

$$\tilde{N} = \begin{cases} \Gamma^{(o_{n_o})} \cup \bar{\mathcal{S}}_{b_0}^{(o_m)} & \text{if } c_j = b_0^{(o_m)}, \\ & m \in \{1, \dots, n_o\} \\ \bigcup_{\ell=1}^{n_o} b_0^{(o_\ell)} & \text{if } c_j \in \Gamma^{(o_{n_o})} \\ \{b_0^{(o_m)}\} & \text{if } c_j \in \bar{\mathcal{S}}_{b_0}^{(o_m)}, \\ & m \in \{1, \dots, n_o\} \end{cases}. \quad (18)$$

Whereas the updated depolarizing map associated with a noisy orchestration qubit $o_i \in V_o$ is:

$$\begin{aligned} \tilde{\mathcal{D}}_{o_i}(\varrho) = & p\varrho + \frac{(1-p)}{2} \cdot \\ & \left[\varrho + \left(Z_{b_0^{(o_i)}} \prod_{k \in \tilde{N}} Z_k \right) \varrho \left(Z_{b_0^{(o_i)}} \prod_{k \in \tilde{N}} Z_k \right) \right], \end{aligned} \quad (19)$$

where the post-measurement neighborhood \tilde{N} is given by: $\tilde{N} = \bigcup_{\ell=i+1}^{n_o} \{b_0^{(o_\ell)}\}$, which is empty ($\tilde{N} = \emptyset$) for $o_i = o_{n_o}$.

Proof. Please refer to Appendix C for the proof. \square

The order of Pauli- X measurements affects the resulting noise maps. We assumed the left-to-right ordering $\{o_1, \dots, o_{n_o}\}$, without loss of generality, since other orderings follow by relabeling. In the worst-case regime where all n qubits are affected by noise, the final noisy state is obtained by composing the updated local maps over all the qubits, i.e., $\tilde{\mathcal{D}}_1 \tilde{\mathcal{D}}_2 \dots \tilde{\mathcal{D}}_n |G\rangle \langle G|$.

B. Fidelity of Noisy Entanglement Resources

We now quantify the fidelity of the entanglement resources instantiated by whatever-channel resolution under noise. In the considered two-stage procedure, Entanglement Rolling selects a target entanglement-graph configuration, and local Pauli- Z measurements at Tier1 nodes isolate disjoint resources from the instantiated configuration, as illustrated in Figs. 4 and 5a. Building on the closed-form updated noise maps derived in Prop. 1, we evaluate how depolarizing noise impacts GTL resource states and compute the fidelities⁴ for representative instantiated resources (Bell pairs and GHZ states).

As depicted in Fig. 5a, we consider the GTL graph state $(G, \hat{\kappa}_b = 2)$ with $n_o = 3$. By applying a two-stage resolution, it is possible to extract up to 3 independent Bell pairs between end nodes. Moreover, in Fig. 5b, we plot the fidelity of each

extracted Bell pair with respect to the depolarizing noise parameter p .

To better describe the fidelity of the resulting states, we also take into account time-dependent dephasing noise:

$$\mathcal{F}(t) = (1 - q(t))\varrho + q(t)Z\varrho Z, \quad (20)$$

where $q(t) = \frac{1}{2}(1 - e^{-t/T})$ estimates the probability of a phase-flip error after a time t , and T is the characteristic dephasing time of the quantum memory. Hence, the noise maps for each qubit j of the graph state are given by the composition of the two noise channels, i.e., $\mathcal{F}_j(t)\mathcal{D}_j$. Therefore, the resulting noisy graph state is given by: $\mathcal{F}_1(t)\mathcal{D}_1 \dots \mathcal{F}_n(t)\mathcal{D}_n |G\rangle \langle G|$.

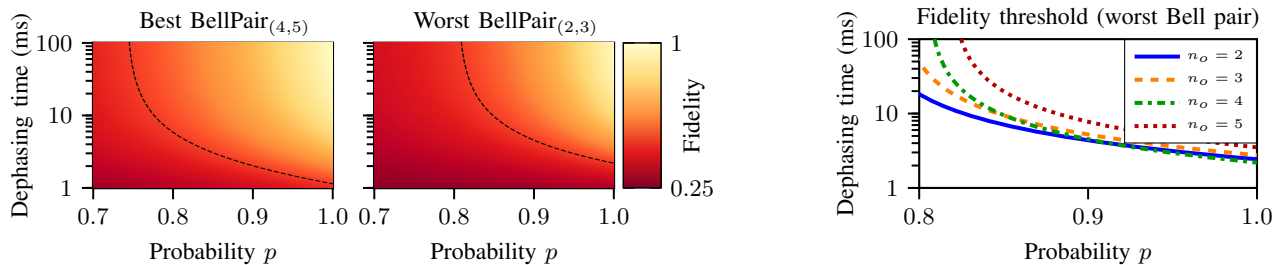
We present additional simulation results in Fig. 6, by taking into account both depolarizing and time-dependent dephasing noise. In particular, in Fig. 6a, we consider a GTL graph state $(G, \hat{\kappa}_b = 2)$ with $n_o = 4$, capable of extracting up to 4 Bell pairs in the presence of both depolarizing and time-dependent dephasing noise. Specifically, we plot the fidelity of the extracted Bell pairs as a function of both the depolarizing parameter p and the dephasing time T . To perform this experiment we considered a total protocol completion time compatible with [48]. The end of the manipulation protocol is at 1 ms, when the last qubit is measured and the classical corrections performed. The total elapsed time determines the accumulated dephasing, while the order of Pauli X measurements affects the noise map updates.

Similarly, Fig. 6b considers a GTL graph state $(G, \hat{\kappa}_b = 3)$ with $n_o = 4$, which can instantiate up to 4 three-qubit GHZ states. We observe higher fidelity when the extracted resources involve Tier1 endpoints located in the ‘‘central’’ part of the entanglement structure, as opposed to the external endpoints. This is due to the fact that the noise maps of the qubits in the middle of the structure are adjacent to more orchestration qubits, thus causing favorable simplifications on the updated noise maps. In both configurations, the fidelity remains above the reference threshold of $F=0.5$ across a broad range of noise parameters [51]. This value is adopted as a benchmark and lies above the minimum threshold required for GHZ state distillation [52]. Regions where the fidelity drops below this threshold are indicated by the dashed black contour in Figs. 6a and 6b, confirming the resilience of the proposed entanglement manipulation framework. As expected, increasing n_o tightens the admissible noise regime, since longer measurement sequences and longer memory times exacerbate error accumulation. Nonetheless, even for $n_o = 5$, a substantial above-threshold region persists, indicating that the framework remains viable at larger scales under realistic noise budgets.

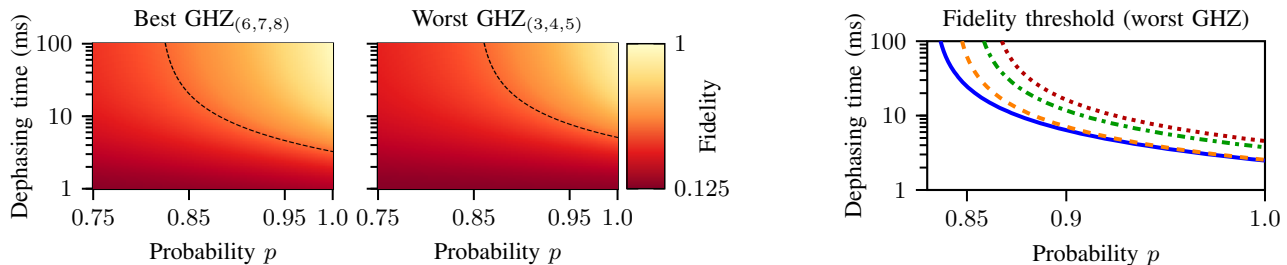
VII. CONCLUSION

In this work, we introduced a resource-driven framework for the programmable reconfiguration of multipartite entanglement, in line with the entanglement-defined networking vision underpinning emerging Quantum Internet architectures and protocol suites [1], [2]. Rather than viewing entanglement manipulation solely as a tool to satisfy predefined connectivity requests, we modeled a shared multipartite entangled state

⁴The numerical validation of the theoretical findings and the final-state fidelity are performed by using the NSF simulation tool, available at [50].



(a) Extracted Bell-pair fidelity from GTL = $(G, \hat{\kappa}_b=2)$ and $n_o=4$: best pair (left) and worst pair (right). (c) Fidelity $F=0.5$ threshold for Bell-pair extraction from GTL = $(G, \hat{\kappa}_b=2)$ with $n_o \in \{2, 3, 4, 5\}$.



(b) Extracted GHZ-state fidelity from GTL = $(G, \hat{\kappa}_b=3)$ and $n_o=4$: best triple (left) and worst triple (right). (d) Fidelity $F=0.5$ threshold for GHZ-state extraction from GTL = $(G, \hat{\kappa}_b=3)$ with $n_o \in \{2, 3, 4, 5\}$.

Fig. 6: Simulation of noisy entanglement extraction under depolarizing and time-dependent dephasing noise. Figs. 6a and 6b represent fidelity heatmaps for $n_o=4$ GTL resource states. The dashed black contour marks the $F=0.5$ threshold. Figs. 6c and 6d represent $F=0.5$ noise threshold curves for different GTL resource states with $n_o \in \{2, 3, 4, 5\}$.

as a *whatever channel*, that can be systematically resolved via LOCC into different entanglement-connectivity configurations, from an admissible configuration space. Focusing on the GTL family, we formalized Entanglement Rolling as a measurement-based mechanism that systematically navigates this space. We proved that for GTL graph states with $\hat{\kappa}_b \geq 2$, the procedure attains the maximum number of concurrently instantiable Bell pairs. Using the Noisy Stabilizer Formalism, we derived closed-form updated noise maps for Entanglement Rolling and the subsequent isolation steps, and evaluated performance under depolarizing and time-dependent dephasing noise. Across a broad range of noise parameters, the resulting Bell-pair and GHZ-state fidelities remain above the threshold $F = 0.5$, supporting the practical viability of the proposed approach.

APPENDIX A PROOF OF THEOREM 1

We assume that a Pauli X measurement is performed on orchestration qubit $o_i \in V_o$ and with corresponding i -th support vertex $b_0^{(o_i)}$ selected to be a right bridge for every measured qubit: $b_0^{(o_i)} = \bar{r} \in \mathcal{R}_B^{(o_i)}$. As the choice is arbitrary, the proof can be carried similarly by choosing $b_0^{(o_i)} = \bar{\ell} \in \mathcal{L}_B^{(o_i)}$.

When performing a Pauli X measurement the effects on the resulting graph state – up to local corrections – are given by the graph $\tau_{b_0}(\tau_{o_i}(\tau_{b_0}(G) - o_i))$. Specifically, after the local complementation $\tau_{b_0}(G)$, the resulting associated graph $G' = (V', E')$ can be expressed as follows:

$$G' = \begin{cases} (V, E \cup \{o_i, o_{i+1}\}) & \text{if } i < n_o \\ (V, E) & \text{if } i = n_o \end{cases}. \quad (21)$$

Moreover, starting from the graph G' another local complementation $\tau_{o_i}(G')$ is performed leading to the graph G'' whose edge set E'' is given by:

$$E'' = (E' \cup N_{o_i}'^2) \setminus E_{N_{o_i}'}, \quad (22)$$

where, according to Eq. (21) the neighborhood N_{o_i}' includes the subsequent orchestration qubit o_{i+1} , if $i < n_o$. Therefore, each peer adjacent to o_i becomes now adjacent also to o_{i+1} . This is given by the union of E' with the set $N_{o_i}'^2$, that is:

$$N_{o_i}'^2 = \begin{cases} (\{o_{i+1}\} \times N_{o_i}) \cup (N_{o_i} \times N_{o_i}) & \text{if } i < n_o \\ N_{o_i} \times N_{o_i} & \text{if } i = n_o \end{cases}. \quad (23)$$

Accordingly, $E_{N_{o_i}'}$ includes the pre-existing edges between o_{i+1} and the right bridges $\mathcal{R}_B^{(o_i)}$, i.e., every link of the kind $\{o_{i+1}, r\}, \forall r \in \mathcal{R}_B^{(o_i)}$.

As a consequence, these links are removed from E'' leading to the disconnections of the bridges $\mathcal{R}_B^{(o_i)}$ from orchestration qubit o_{i+1} , if any. Formally:

$$E_{N_{o_i}'} = \begin{cases} \{\{o_{i+1}, r\} : r \in \mathcal{R}_B^{(o_i)}\} & \text{if } i < n_o \\ \emptyset & \text{if } i = n_o \end{cases}. \quad (24)$$

Furthermore, when o_i is removed the resulting graph G''' can be expressed as follows:

$$G''' = (V \setminus \{o_i\}, E'' \setminus (\{o_i\} \times N_{o_i})). \quad (25)$$

The last local complementation is, once again, applied on $b_0^{(o_i)}$. This leads to the graph G^{IV} , whose edge set is given by:

$$E^{IV} = (E''' \cup N_{b_0}'''^2) \setminus E_{N_{b_0}'''} \quad (26)$$

It is worth noting that $N_{b_0}'''^2$ contains every possible edge between vertices adjacent to $b_0^{(o_i)}$. However, according to Eq. (23), all those edges are already contained in $N_{o_i}'^2$ since $b_0^{(o_i)} \in N_{o_i}'$. Therefore, we have that $E''' \cup N_{b_0}'''^2 = E'''$. Moreover, $E_{N_{b_0}''}'$ contains every edge whose end-points are not $b_0^{(o_i)}$ nor o_{i+1} . This is because, according to Eq. (23) and Eqs. (22)-(24) we have: $o_{i+1} \in N_{o_i}' \wedge o_{i+1} \notin N_{b_0}'''$.

As a consequence, every edge contained in $N_{o_i}'^2$ without $b_0^{(o_i)}$ as one of the endpoints is canceled. This means that the neighborhood of the support vertex after all the local complementations is given by:

$$N_{b_0^{(o_i)}}^{IV} = N_{o_i} \setminus \{b_0^{(o_i)}\}, \quad (27)$$

and its edge set is exactly given by $N_{o_i}: E^{IV} = \{b_0^{(o_i)}\} \times N_{o_i}$. Hence, since no more edges are present between the vertices of the set $N_{o_i} \setminus \{b_0^{(o_i)}\}$, the current support vertex $b_0^{(o_i)}$ is also a star vertex for each of its neighbors, satisfying point I of the theorem.

According to Eq. (22), every non $b_0^{(o_i)}$ right bridge (i.e., $\hat{b} \in \mathcal{R}_{b_0}^{(o_i)}$) is no longer connected to o_{i+1} , thus losing its bridge role: $N_{\hat{b}}^{IV} = b_0^{(o_i)}, \forall \hat{b} \in \mathcal{R}_{b_0}^{(o_i)}$. Conversely, we denote the remaining qubits of the pre-measurement neighborhood N_{o_i} as $\gamma \in \Gamma$, which are non bridge and non support qubits, i.e. $\gamma \notin \mathcal{R}_B^{(o_i)} \wedge \gamma \neq b_0^{(o_i)}, \forall \gamma \in \Gamma$. Moreover, according to Eqs. (22)-(23) we have that $\Gamma = N_{o_i} \setminus \mathcal{R}_B^{(o_i)}$ with neighborhood:

$$N_{\gamma}^{IV} = \begin{cases} (N_{\gamma} \setminus \{o_i\}) \cup \{b_0^{(o_i)}, o_{i+1}\} & \text{if } i < n_o \\ (N_{\gamma} \setminus \{o_i\}) \cup \{b_0^{(o_i)}\} & \text{if } i = n_o \end{cases} \quad (28)$$

This means that each qubit $\gamma \in \Gamma$ has a direct link to $b_0^{(o_i)}$ and o_{i+1} , if any. In other words, the set of vertices Γ replaces the set $\mathcal{R}_B^{(o_i)}$ in the resulting graph and becomes left bridge set $\mathcal{L}_B^{(o_{i+1})}$ for the subsequent orchestration qubit o_{i+1} , if any. Hence, point II follows.

APPENDIX B PROOF OF COROLLARY 2

By applying Th. 1 at each of the n_o orchestration qubits in sequence, each $b_0^{(o_i)}$ vertex acquires the neighborhood given by Eq. (27), with no edges among its neighbors. Specifically, every non $b_0^{(o_i)}$ right bridge $\hat{b} \in \mathcal{R}_{b_0}^{(o_i)}$ is no longer connected to any orchestration qubit, thus losing its bridge role according to Th. 1. The total number of these vertices is:

$$|\mathcal{R}_{b_0}^{(o_i)}| = \hat{\kappa}_b - 1, \quad \forall o_i \in V_o, \quad (29)$$

independently of the choice of the support vertex $b_0^{(o_i)}$ at each measurement step i , since $|\mathcal{R}_B^{(o_i)}| = \hat{\kappa}_b$ by C3 of Def. 5.

By Eq. (28) and induction on the measurement steps (since $\Gamma^{(o_i)}$ becomes $\mathcal{L}_B^{(o_{i+1})}$ at each step, acquiring a new link to

$b_0^{(o_{i+1})}$), the rolled set $\Gamma^{(o_{n_o})}$, with $|\Gamma^{(o_{n_o})}| = \kappa_c - \hat{\kappa}_b$, is connected to every designated $b_0^{(o_i)} \in \mathcal{S}_{b_0}$:

$$N_{\Gamma^{(o_{n_o})}} = \{b_0^{(o_1)}, b_0^{(o_2)}, \dots, b_0^{(o_{n_o})}\} = \mathcal{S}_{b_0}, \quad (30)$$

and each designated b_0 vertex is connected to:

$$N_{b_0^{(o_i)}} = \mathcal{R}_{b_0}^{(o_i)} \cup \Gamma^{(o_{n_o})}, \quad \forall b_0^{(o_i)} \in \mathcal{S}_{b_0}. \quad (31)$$

Hence, by performing a Pauli-Z measurement on each of the vertices $\gamma \in \Gamma^{(o_{n_o})}$, the neighborhood of each designated $b_0^{(o_i)}$ vertex is updated as follows:

$$N_{b_0^{(o_i)}}' = \mathcal{R}_{b_0}^{(o_i)}, \quad \forall b_0^{(o_i)} \in \mathcal{S}_{b_0}. \quad (32)$$

The proof follows by noticing that the resulting graph is a collection of n_o disconnected star graph states, each one centered in a $b_0^{(o_i)}$. Accordingly, being LU equivalent to a GHZ state, each star graph state allows the extraction of a single Bell state between the center $b_0^{(o_i)}$ and one of its adjacent vertices in $\mathcal{R}_{b_0}^{(o_i)}$ by performing Pauli Z measurements on the remaining $\hat{\kappa}_b - 2$ leaves ($\hat{\kappa}_b - 2$ measurements per star, $n_o(\hat{\kappa}_b - 2)$ in total).

To show that n_o is also the theoretical maximum number of instantiable Bell states in the operating regime of $\hat{\kappa}_b \geq 2$, we refer to the Schmidt Measure $\mathbf{P}(|G\rangle)$ of a graph state $|G\rangle$ [53]. Specifically, for a two-colorable graph state $|G\rangle$ with associated graph $G = (V, E)$ and vertex set $V = V_o \cup V_c$ the following bounds hold [41]:

$$\frac{1}{2} \text{rank}(\Gamma_G) \leq \mathbf{P}(|G\rangle) \leq \min\{|V_o|, |V_c|\}, \quad (33)$$

where $\text{rank}(\Gamma_G)$ represents the rank of the adjacency matrix of the graph G and $\mathbf{P}(|G\rangle)$ is the Schmidt Measure of the graph state $|G\rangle$. Accordingly, the Schmidt rank has a closed form for the initial GTL resource state. Specifically half of the rank of the adjacency matrix and the cardinality of the orchestration vertex set $|V_o|$ coincide and are equal to n_o [29]. Since the number of Bell states can not exceed $\mathbf{P}(|G\rangle) = n_o$, the number of extractable Bell states is also the maximum.

APPENDIX C PROOF OF PROPOSITION 1

Let us consider the ordered Pauli-X measurement sequence $\mathcal{O}_x = \{\mathbf{M}_{x,\pm}^{(o_1)}, \mathbf{M}_{x,\pm}^{(o_2)}, \dots, \mathbf{M}_{x,\pm}^{(o_{n_o})}\}$ acting on the orchestration qubits of the GTL resource state. We analyze a generic peer qubit $c_j \in V_c$ adjacent to an orchestration qubit $o_i \in V_o$ and derive the corresponding NSF-updated depolarizing noise map after commuting local depolarizing noise through \mathcal{O}_x . We recall that, the set of rolled vertices $\Gamma^{(o_m)}$, $m \in \{1, \dots, n_o\}$, can be updated at each measurement step, thus the support vertex $b_0^{(o_m)}$ can be chosen as left or right bridge accordingly. Hence, the set of non- b_0 vertices at measurement stage m can be expressed according to Eq. (14).

When an orchestration qubit o_{i-1} (if any) is measured in the X basis, the map of qubit c_j is updated according to the neighborhood of the measured vertex. According to Tab. I,

there are two possible update rules for the depolarizing map on c_j :

$$\mathbf{M}_{x,\pm}^{(o_{i-1})} \rightarrow \tilde{\Lambda} = \begin{cases} Z_{c_j}^\beta \prod_{k \in N'_{c_j}} Z_k^\alpha & \text{if } c_j = b_0^{(o_{i-1})} \\ Z_{c_j}^\alpha \prod_{k \in N'_{c_j}} Z_k^\beta & \text{otherwise} \end{cases}. \quad (34)$$

For any previous measurement step whose measured vertex is not adjacent to c_j , the map is unchanged. When qubit o_{i-1} is measured, the depolarizing noise map is then updated as:

$$\tilde{\mathcal{D}}_{c_j}^{(o_{i-1})}(\varrho) = p\varrho + \frac{(1-p)}{4} \begin{cases} \sum_{\alpha,\beta \in \{0,1\}} (Z_{c_j}^\beta \prod_{k \in \tilde{N}} Z_k^\alpha) \varrho (Z_{c_j}^\beta \prod_{k \in \tilde{N}} Z_k^\alpha) & \text{if } c_j = b_0^{(o_{i-1})} \\ \sum_{\alpha,\beta \in \{0,1\}} (Z_{c_j}^\alpha \prod_{k \in \tilde{N}} Z_k^\beta) \varrho (Z_{c_j}^\alpha \prod_{k \in \tilde{N}} Z_k^\beta) & \text{otherwise} \end{cases}, \quad (35)$$

where the post-measurement neighborhood \tilde{N} is given accordingly to Th. 1:

$$\tilde{N} = \begin{cases} \Gamma^{(o_{i-1})} \cup \bar{\mathcal{S}}_{b_0}^{(o_{i-1})} & \text{if } c_j = b_0^{(o_{i-1})} \\ \{o_i\} \cup \bigcup_{\ell=1}^{i-1} \{b_0^{(o_\ell)}\} & \text{if } c_j \in \Gamma^{(o_{i-1})} \\ \{b_0^{(o_{i-1})}\} & \text{if } c_j \in \bar{\mathcal{S}}_{b_0}^{(o_{i-1})} \end{cases}. \quad (36)$$

When the considered o_i qubit is measured, the noisy operator updates according to the same rules above. Notably, if $c_j \notin \Gamma^{(o_m)}$, $m \in \{i, \dots, n_o\}$, its map is no longer updated, according to the resulting post-measurement neighborhood. Consequently, the depolarizing map is updated as follows:

$$\mathcal{D}_{c_j}^{(o_i)}(\varrho) = p\varrho + \frac{(1-p)}{4} \begin{cases} \sum_{\alpha,\beta \in \{0,1\}} (Z_{c_j}^\beta \prod_{k \in \tilde{N}} Z_k^\alpha) \varrho (Z_{c_j}^\beta \prod_{k \in \tilde{N}} Z_k^\alpha) & \text{if } c_j = b_0^{(o_i)} \\ \sum_{\alpha,\beta \in \{0,1\}} (Z_{c_j}^\alpha \prod_{k \in \tilde{N}} Z_k^\beta) \varrho (Z_{c_j}^\alpha \prod_{k \in \tilde{N}} Z_k^\beta) & \text{otherwise} \end{cases}, \quad (37)$$

where the post-measurement neighborhood \tilde{N} is updated accordingly:

$$\tilde{N} = \begin{cases} \Gamma^{(o_i)} \cup \bar{\mathcal{S}}_{b_0}^{(o_m)} & \text{if } c_j = b_0^{(o_m)}, \\ & m \in \{i-1, \dots, n_o\} \\ \{o_{i+1}\} \cup \bigcup_{\ell=1}^i \{b_0^{(o_\ell)}\} & \text{if } c_j \in \Gamma^{(o_i)} \\ \{b_0^{(o_m)}\} & \text{if } c_j \in \bar{\mathcal{S}}_{b_0}^{(o_m)}, \\ & m \in \{i-1, i\} \end{cases}. \quad (38)$$

By applying the same update rules until the last measurement, and by noting that $\{\beta, \alpha\}$ can be relabeled as $\{\alpha, \beta\}$ without loss of generality, the overall noise map on peer qubit c_j is given by:

$$\tilde{\mathcal{D}}_{c_j}(\varrho) = p\varrho + \frac{(1-p)}{4} \sum_{\alpha,\beta \in \{0,1\}} (Z_{c_j}^\alpha \prod_{k \in \tilde{N}} Z_k^\beta) \varrho (Z_{c_j}^\alpha \prod_{k \in \tilde{N}} Z_k^\beta) \quad (39)$$

where the post-measurement neighborhood \tilde{N} is given by:

$$\tilde{N} = \begin{cases} \Gamma^{(o_{n_o})} \cup \bar{\mathcal{S}}_{b_0}^{(o_m)} & \text{if } c_j = b_0^{(o_m)}, \\ & m \in \{1, \dots, n_o\} \\ \bigcup_{\ell=1}^{n_o} b_0^{(o_\ell)} & \text{if } c_j \in \Gamma^{(o_{n_o})} \\ \{b_0^{(o_m)}\} & \text{if } c_j \in \bar{\mathcal{S}}_{b_0}^{(o_m)}, \\ & m \in \{1, \dots, n_o\} \end{cases}. \quad (40)$$

By expanding the coefficients, the full expression of the final noise map is as follows:

$$\tilde{\mathcal{D}}_{c_j}(\varrho) = p\varrho + \frac{(1-p)}{4} [\varrho + Z_{c_j} \varrho Z_{c_j} + (\prod_{k \in \tilde{N}} Z_k) \varrho (\prod_{k \in \tilde{N}} Z_k) + (Z_{c_j} \prod_{k \in \tilde{N}} Z_k) \varrho (Z_{c_j} \prod_{k \in \tilde{N}} Z_k)]. \quad (41)$$

The same approach can be carried on for the depolarizing noise map of each orchestration qubit $o_i \in V_o$. If o_{i-1} is measured, its noise map is updated according to Tab. I as follows:

$$\tilde{\mathcal{D}}_{o_i}^{(o_{i-1})}(\varrho) = p\varrho + \frac{(1-p)}{4} \sum_{\alpha,\beta \in \{0,1\}} (Z_{o_i}^\alpha \prod_{k \in \tilde{N}} Z_k^\beta) \varrho (Z_{o_i}^\alpha \prod_{k \in \tilde{N}} Z_k^\beta), \quad (42)$$

where, regardless of the arbitrary choice of $\Gamma^{(o_{i-1})}$ as left or right bridge set, the post-measurement neighborhood \tilde{N} is given by:

$$\tilde{N} = (N_{o_i} \setminus \mathcal{L}_B^{(o_i)}) \cup \Gamma^{(o_{i-1})}. \quad (43)$$

When o_i is measured, its noise map is then updated as:

$$\tilde{\mathcal{D}}_{o_i}^{(o_i)}(\varrho) = p\varrho + \frac{(1-p)}{4} \sum_{\alpha \in \{0,1\}} (Z_{b_0^{(o_i)}}^\alpha \prod_{k \in N_{b_0}^{(o_i)}} Z_k^\alpha) \varrho (Z_{b_0^{(o_i)}}^\alpha \prod_{k \in N_{b_0}^{(o_i)}} Z_k^\alpha), \quad (44)$$

where the pre-measurement neighborhood $N_{b_0}^{(o_i)}$ is:

$$N_{b_0}^{(o_i)} = \begin{cases} \{o_i\} \cup \{o_{i+1}\} & \text{if } b_0^{(o_i)} \in \mathcal{R}_B^{(o_i)} \quad (o_i \neq o_{n_o}) \\ \{o_i\} & \text{if } b_0^{(o_i)} \in \mathcal{R}_B^{(o_i)} \quad (o_i = o_{n_o}) \\ \{b_0^{(o_{i-1})}\} \cup \{o_i\} & \text{if } b_0^{(o_i)} \in \mathcal{L}_B^{(o_i)} \end{cases}. \quad (45)$$

When qubit o_i is removed from the system, the effective noise operator on o_i reduces to: $Z_{b_0^{(o_i)}}^\alpha \prod_{k \in N_{b_0}^{(o_i)} \setminus \{o_i\}} Z_k^\alpha$. In the following we focus on the case $b_0^{(o_i)} \in \mathcal{R}_B^{(o_i)}$ and $b_0^{(o_i)} \in \mathcal{L}_B^{(o_i)}$ follows symmetrically. Eq. (45) gives $N_{b_0}^{(o_i)} \setminus \{o_i\} = \{o_{i+1}\}$ (if any o_{i+1}), so the residual operator is $Z_{b_0^{(o_i)}}^\alpha Z_{o_{i+1}}^\alpha$. Instead, when o_{i+1} is measured the operator $Z_{o_{i+1}}^\alpha$ updates as: $Z_{o_{i+1}}^\alpha \mapsto Z_{b_0^{(o_{i+1})}}^\alpha Z_{o_{i+1}}^\alpha Z_{o_{i+2}}^\alpha$. Thus, the operator for o_i becomes $Z_{b_0^{(o_i)}}^\alpha Z_{b_0^{(o_{i+1})}}^\alpha Z_{o_{i+2}}^\alpha$. By iterating these steps, no residual factor remains after the last measurement, hence the

final operator is $Z_{b_0^{(o_i)}}^\alpha Z_{b_0^{(o_{i+1})}}^\alpha \cdots Z_{b_0^{(o_{n_o})}}^\alpha$, corresponding to the final noise map is given by:

$$\tilde{D}_{o_i}(\varrho) = p\varrho + \frac{(1-p)}{2} \left[\varrho + \left(Z_{b_0^{(o_i)}} \prod_{k \in N_{b_0}^{(o_i)}} Z_k \right) \varrho \left(Z_{b_0^{(o_i)}} \prod_{k \in N_{b_0}^{(o_i)}} Z_k \right) \right], \quad (46)$$

and the final post-measurement neighborhood $N_{b_0}^{(o_i)}$ is simply $N_{b_0}^{(o_i)} = \bigcup_{\ell=i+1}^{n_o} \{b_0^{(o_\ell)}\}$, which is empty ($N_{b_0}^{(o_{n_o})} = \emptyset$) for $o_i = o_{n_o}$, according to Eq. (45). This concludes the proof.

REFERENCES

- [1] A. S. Cacciapuoti and M. Caleffi, "A quantum internet protocol suite beyond layering," *IEEE TNSE*, 2026. invited paper.
- [2] M. Caleffi and A. S. Cacciapuoti, "Quantum Internet Architecture: unlocking Quantum-Native Routing via Quantum Addressing," *IEEE Transactions on Communications*, 2026. invited paper.
- [3] A. S. Cacciapuoti, M. Caleffi, J. Illiano, C. D. Risi, A. Abane, and J. Chung, "Quantum-Native Architectural Tenets and Philosophy for the Quantum Internet," Internet-Draft draft-cacciapuoti-qirg-quantum-native-architecture-01, Internet Engineering Task Force, Apr. 2026. Work in Progress.
- [4] H. J. Kimble, "The quantum internet," *Nature*, vol. 453, no. 7198, pp. 1023–1030, 2008.
- [5] W. Dür, R. Lamprecht, and S. Heusler, "Towards a quantum internet," *European Journal of Physics*, vol. 38, no. 4, p. 043001, 2017.
- [6] A. S. Cacciapuoti, M. Caleffi, R. Van Meter, and L. Hanzo, "When entanglement meets classical communications: Quantum teleportation for the quantum internet," *IEEE TCOM*, vol. 68, no. 6, pp. 3808–3833, 2020. invited paper.
- [7] K. Azuma, S. E. Economou, D. Elkouss, *et al.*, "Quantum repeaters: From quantum networks to the quantum internet," *Rev. Mod. Phys.*, vol. 95, p. 045006, Dec 2023.
- [8] A. Pirker and W. Dür, "A quantum network stack and protocols for reliable entanglement-based networks," *New Journal of Physics*, vol. 21, p. 033003, mar 2019.
- [9] J. I. Cirac, A. K. Ekert, S. F. Huelga, *et al.*, "Distributed quantum computation over noisy channels," *Phys. Rev. A*, vol. 59, pp. 4249–4254, Jun 1999.
- [10] M. Hayashi and T. Morimae, "Verifiable measurement-only blind quantum computing with stabilizer testing," *Phys. Rev. Lett.*, vol. 115, p. 220502, Nov 2015.
- [11] M. Caleffi, M. Amoretti, D. Ferrari, J. Illiano, A. Manzalini, and A. S. Cacciapuoti, "Distributed quantum computing: A survey," *Computer Networks*, vol. 254, p. 110672, 2024.
- [12] N. Gisin, G. Ribordy, W. Tittel, *et al.*, "Quantum cryptography," *Rev. Mod. Phys.*, vol. 74, pp. 145–195, Mar 2002.
- [13] S. Pirandola, U. L. Andersen, L. Banchi, *et al.*, "Advances in quantum cryptography," *Advances in Optics and Photonics*, vol. 12, p. 1012, Dec. 2020.
- [14] V. Giovannetti, S. Lloyd, and L. Maccone, "Advances in quantum metrology," *Nature Photonics*, vol. 5, pp. 222–229, Mar. 2011.
- [15] E. M. Kessler, I. Lovchinsky, A. O. Sushkov, *et al.*, "Quantum error correction for metrology," *Phys. Rev. Lett.*, vol. 112, p. 150802, Apr 2014.
- [16] P. Sekatski, S. Wölk, and W. Dür, "Optimal distributed sensing in noisy environments," *Phys. Rev. Research*, vol. 2, p. 023052, Apr 2020.
- [17] A. Giani, M. Z. Win, and A. Conti, "Quantum sensing and communication via non-gaussian states," *IEEE JSAT*, vol. 6, pp. 18–33, 2025.
- [18] R. Jozsa and N. Linden, "On the role of entanglement in quantum-computational speed-up," *Proc. R. Soc of London. A*, vol. 459, no. 2036, pp. 2011–2032, 2003.
- [19] G. Avis, F. Rozpędek, and S. Wehner, "Analysis of multipartite entanglement distribution using a central quantum-network node," *Phys. Rev. A*, vol. 107, p. 012609, Jan 2023.
- [20] Á. G. Iñesta *et al.*, "Optimal entanglement distribution policies in homogeneous repeater chains with cutoffs," *npj Quantum Info.*, vol. 9, no. 1, p. 46, 2023.
- [21] J. Chung *et al.*, "Orchestration of Entanglement Distribution over a Q-LAN using the IEQNET Controller," in *OFC*, 2024.
- [22] A. Abane *et al.*, "Entanglement routing in quantum networks: A comprehensive survey," *IEEE TQE*, vol. 6, pp. 1–39, 2025.
- [23] J. I. Cirac, P. Zoller, H. J. Kimble, *et al.*, "Quantum state transfer and entanglement distribution among distant nodes in a quantum network," *Phys. Rev. Lett.*, vol. 78, no. 16, p. 3221, 1997.
- [24] A. S. Cacciapuoti, J. Illiano, and M. Caleffi, "Quantum internet addressing," *IEEE Network*, pp. 1–1, 2023.
- [25] J. Miguel-Ramiro, A. Pirker, and W. Dür, "Genuine quantum networks with superposed tasks and addressing," *npj Quantum Info.*, vol. 7, p. 135, 2021.
- [26] J. Illiano, M. Caleffi, *et al.*, "Quantum MAC: Genuine entanglement access control via many-body dicke states," *IEEE TCOM*, 2023.
- [27] J. Illiano, M. Caleffi, A. Manzalini, and A. S. Cacciapuoti, "Quantum internet protocol stack: a comprehensive survey," *Computer Networks*, vol. 213, 2022.
- [28] S.-Y. Chen, A. S. Cacciapuoti, and M. Caleffi, "Quantum routing beyond pathfinding: Multipartite entanglement complementation," 2026.
- [29] F. Mazza, M. Caleffi, and A. S. Cacciapuoti, "Intra-qlan connectivity via graph states: Beyond the physical topology," *IEEE TNSE*, 2025.
- [30] M. F. Mor-Ruiz and W. Dür, "Noisy stabilizer formalism," *Physical Review A*, vol. 107, no. 3, p. 032424, 2023.
- [31] P. Aigner, M. F. Mor-Ruiz, and W. Dür, "Qudit noisy stabilizer formalism," *Phys. Rev. A*, vol. 112, p. 022402, Aug 2025.
- [32] Buterakos, Donovan and Barnes, Edwin and Economou, Sophia E., "Deterministic generation of all-photon quantum repeaters from solid-state emitters," *Phys. Rev. X*, vol. 7, p. 041023, Oct 2017.
- [33] A. Russo, E. Barnes, and S. E. Economou, "Generation of arbitrary all-photon graph states from quantum emitters," *New Journal of Physics*, vol. 21, no. 5, p. 055002, 2019.
- [34] P. Thomas *et al.*, "Efficient generation of entangled multiphoton graph states from a single atom," *Nature*, vol. 608, no. 7924, pp. 677–681, 2022.
- [35] P. Thomas *et al.*, "Fusion of deterministically generated photonic graph states," *Nature*, vol. 629, pp. 567–572, 2024.
- [36] Y. Meng *et al.*, "Temporal fusion of entangled resource states from a quantum emitter," *Nature Communications*, vol. 16, no. 1, p. 7602, 2025.
- [37] K. Azuma, K. Tamaki, and H.-K. Lo, "All-photon quantum repeaters," *Nature communications*, vol. 6, no. 1, p. 6787, 2015.
- [38] M. F. Mor-Ruiz, J. Miguel-Ramiro, J. Wallnöfer, *et al.*, "Merging-based quantum repeater," *arXiv preprint arXiv:2502.04450*, 2025.
- [39] A. Dahlberg and S. Wehner, "Transforming graph states using single-qubit operations," *Philos. Trans. R. Soc. A*, vol. 376, no. 2123, p. 20170325, 2018.
- [40] A. Dahlberg, J. Helsen, and S. Wehner, "Transforming graph states to bell-pairs is np-complete," *Quantum*, vol. 4, p. 348, 2020.
- [41] M. Hein, J. Eisert, and H. J. Briegel, "Multiparty entanglement in graph states," *Physical Review A*, vol. 69, no. 6, p. 062311, 2004.
- [42] M. Hein *et al.*, "Entanglement in graph states and its applications," 2006.
- [43] F. Hahn, A. Pappa, and J. Eisert, "Quantum network routing and local complementation," *npj Quantum Info.*, vol. 5, no. 1, p. 76, 2019.
- [44] F. Mazza, J. Miguel-Ramiro, J. Illiano, A. Pirker, M. Caleffi, A. S. Cacciapuoti, and W. Dür, "Flexible qubit allocation of network resource states," *arXiv preprint arXiv:2510.15776*, 2025.
- [45] D. Bhatti and K. Goodenough, "Distributing graph states with a photon-weaving quantum server," *arXiv preprint arXiv:2504.07410*, 2025.
- [46] J. Miguel-Ramiro, J. Illiano, F. Mazza, A. Pirker, J. Freund, A. S. Cacciapuoti, M. Caleffi, and W. Dür, "Qping: a quantum ping primitive for quantum networks," *IEEE JSAC*, 2026.
- [47] F. Mazza, C. Zhan, J. Chung, R. Kettimuthu, M. Caleffi, and A. S. Cacciapuoti, "Simulation of Entanglement-Enabled Connectivity in QLANs using SeQuENCe," in *IEEE ICC 2025*, 2025.
- [48] A. Pearson, F. Mazza, M. Caleffi, and A. S. Cacciapuoti, "An extensible quantum network simulator built on ns-3: Q2ns design and evaluation," *Computer Networks*, p. 112292, 2026.
- [49] M. F. Mor-Ruiz, J. Wallnöfer, and W. Dür, "Imperfect quantum networks with tailored resource states," *Quantum*, vol. 9, p. 1605, 2025.
- [50] "noisy-graph-states (GitHub) v0.4." https://github.com/jwallnoefer/noisy_graph_states, 2025.
- [51] C. H. Bennett, *et al.*, "Purification of noisy entanglement and faithful teleportation via noisy channels," *Phys. Rev. Lett.*, vol. 76, pp. 722–725, Jan 1996.
- [52] M.-Z. Zhu and L. Ye, "Efficient entanglement purification for greenberger-horne-zeilinger states via the distributed parity-check detector," *Optics Communications*, vol. 334, pp. 51–57, 2015.
- [53] J. Eisert and H. J. Briegel, "Schmidt measure as a tool for quantifying multiparticle entanglement," *Physical Review A*, vol. 64, July 2001.